

## EXPERIMENTAL AND THEORETICAL STUDY OF THE EXCITED STATE OF 2-ACETYLTHIANTHRENE

Cristina Oncioiu\*, Anca Nicolae\*\* and Mihaela Hillebrand\*

The properties of the excited state of 2-acetylthianthrene (emission maxima, quantum yields, natural lifetime) were investigated in several solvents by means of steady-state fluorescence spectroscopy. The experimental data pointed out a significant bathochromic shift of the emission maxima in polar solvents. Considering the dependence of  $\nu_F$  or  $\Delta\nu_{\text{Stokes}}$  on both the solvent polarity function (Lippert- Mataga model) and the  $E_T^N$  values, the increase in the dipole moment value upon excitation was estimated. The results can be rationalized in terms with a pronounced intramolecular charge transfer character of the first excited state. MO calculations by semiempirical and ab initio methods were performed to support the experimental data.

### Introduction

The aim of the present paper is to discuss the character of the first excited state of 2-acetylthianthrene, **I**, (Fig. 1) in connection with the results previously obtained for two related sulfur containing derivatives, 4-acetyldiphenylsulfide, **II**, and 3-acetylphenoxathiin, **III** [1,2]. For both **II** and **III** the experimental and theoretical data have pointed out that the first singlet is a  $\pi$ - $\pi^*$  excited state and not a  $n$ - $\pi^*$  as would be expected due to the presence of the carbonyl group. The results attested an intramolecular charge transfer (ICT) character of this excited state, the sulphur atom representing the donor center and the acetyl-substituted phenyl moiety, the acceptor part. In the case of the "open" derivative **II**, where the donor and acceptor fragments are joined by a single bond, a change in the excited state conformation occurred leading to a twisted intramolecular charge transfer excited state (TICT). In this state, due to a torsion about the S - substituted phenyl bond, the donor and acceptor parts reached a relative orthogonal position preventing the conjugation. The dipole moment was strongly increased and the solvation process stabilized this state more than the Frank-Condon one. As a result, a dual fluorescence was observed, due to the radiative deactivation of both the Frank-Condon state and the TICT state. As the TICT states are usually nonradiative states for which the nonradiative deactivations pathways are dominating, the quantum yields of **II** were very low especially in polar solvents.

The closure of a median heteroring by an oxygen atom, implying a rigidization of the molecular system strongly modified the emission properties of **III** in comparison with **II**. On the other part, the presence of the acetyl substituent on the phenoxathiin ring determines an enhancement of the fluorescence quantum yield of the parent compound. The dependence of the both the emission maximum and quantum yield of the solvent polarity attests also an ICT character of the first excited singlet.

---

\* Department of Physical Chemistry, Faculty of Chemistry, University of Bucharest, 4-12 Blvd. Elisabeta, Bucharest, Romania

\*\* Department of Organic Chemistry, Faculty of Chemistry, University of Bucharest, Sos. Panduri, Nr. 90-92, Bucharest, Romania

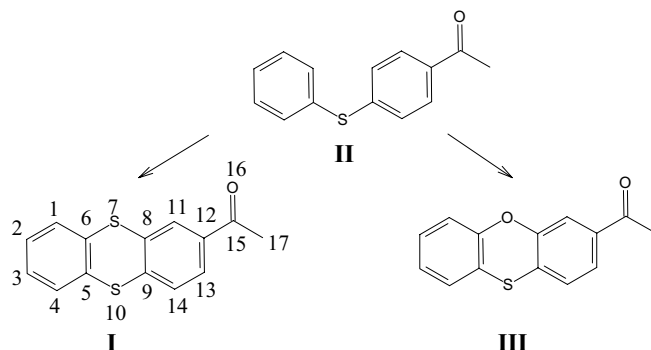


Fig. 1: Structure of the investigated compounds.

It was shown that the acetyl group introduced a low-lying  $\pi$  vacant molecular orbital, located between the frontier orbitals of the parent phenoxathiin. This orbital is mostly localized on the phenyl substituted ring and the acetyl group. The excited state also presents an ICT character but the rigid form of the molecule prevents the conformational transition to a TICT state. Consequently, the quantum yield is higher than that of either II or the unsubstituted phenoxathiin.

In the present case the central bridge between the two phenyl groups is ensured by two sulphur atoms. We will focus on the following points: 1) the influence of the heteroatoms in the median heteroring on the photophysical properties and the character of the first excited singlet; 2) the discussion of the experimental results in terms of the MO calculations for the ground and excited states by both semiempirical and ab initio methods.

## Experimental and Theoretical Methods

2-acetyl-thyanthrene (m.p. in ethanol 85÷86°C) was synthesized by literature methods [5,6]. The absorption spectra and the steady state fluorescence spectra were recorded with a UNICAM - HELLIOS spectrophotometer, and, respectively, with an AMINCO-BOWMAN spectrofluorimeter, using solvents with different polarities. The solvents were Aldrich and Fluka, spectroscopic grade and were checked for fluorescence and used without further purification.

The radiative natural lifetime was estimated using the formula [7]:

$$\tau_0 = \frac{3.417 \cdot 10^8}{\nu_a^2 \cdot n^2 \cdot A}$$

In this relationship  $\nu_a$  represents the wavenumber of the maximum absorption band,  $n$ , the refractive index of the solvent and  $A$  the area of the absorption band,  $\int \epsilon(\nu) d\nu$ . In order to evaluate  $A$ , a deconvolution of the spectra was previously performed in cases of partially overlapping bands. The estimated errors were about 10 percent.

The fluorescence quantum yields,  $\Phi_F$ , were determined relatively to quinine sulphate in 1N  $H_2SO_4$ ,  $\Phi_F = 0.55$ , using the same excitation wavelength,  $\lambda = 320$  nm for the reference and the sample and solutions with absorbance lower than 0.08.

Two other photophysical properties were estimated: the Stokes shift,  $\Delta\nu$  defined as the difference between the absorption and fluorescence maxima,  $\Delta\nu = \nu_A - \nu_F$  and the Stokes loss,  $\Delta\nu_1$ , the difference between the positions of the fluorescence maximum and the 0-0 transition,  $\Delta\nu_1 = \nu_{0,0} - \nu_F$ .

$\nu_{0,0}$  was taken as the point of intersection of the absorption and fluorescence spectra.

The vacuum calculations for ground state ( $S_0$ ) were performed by the semiempirical (AM1) and the ab initio methods (basis STO-3G and STO-321G) using the program GAMESS.[8] The optimisations of the first excited singlet ( $S_1$ ) and triplet ( $T_1$ ) states were carried out using the MOPAC -7 program. Several levels of Configurational Interaction were implied using the key words OPEN(2,2) and C.I.=n. In order to check the charge transfer character of the excited states the calculations were performed in four solvents, cyclohexane (CHX), methanol ( $CH_3OH$ ), acetonitrile (ACN) and dimethylsulphoxyde (DMSO), models for nonpolar, polar protic and polar nonprotic solvents. The calculations including the solvents were performed by the program AMSOL [9,10] using the also AM1 hamiltonian. The solvation model was SM5.1 A. The Eigenvector Following optimization procedure (EF, EFOLLOW) was used in all cases. Although as long as we are aware, the AMSOL program was not used for excited states, we performed calculations using the same key words as for the usual MOPAC calculations, OPEN(2,2), ROOT=2, SINGLET, C.I.=n. The geometry optimisation of the excited states, considering a solvation model was difficult to perform. The minima were flat and the gradients were only about  $1 \div 2$  kcal/  $\text{\AA}^0$  or radian.

Three conformations were considered in respect with the position of the acetyl group defined by the torsion angle  $O_{16}-C_{15}-C_{12}-C_{11}$  (Fig.1), i.e. two in-plane configurations, **I-0** and **I-180** and a twisted one, **I-90**.

## Results and Discussion

In the range 250-350 nm the spectrum of the unsubstituted thianthrene consists in two overlapped intense bands located around 254 nm and a shoulder on the longer wavelength side, at 290 nm. In the same range, 2-acetylthianthrene presents besides the bands found in the parent compound, a third absorption maximum of low intensity at 325-340 nm. This band is like a shoulder on the right side of the band at 300 nm and the exact positions of the maxima listed in Table 1 were obtained by the deconvolution of the spectra. In going from cyclohexane to methanol, the change of the solvent polarity determines a bathochromic shift of the band.

Although the molar absorptivities are small, at the limit between the  $\pi-\pi^*$  and  $n-\pi^*$  values, considering the solvent effect and the similitudes with the other two derivatives we consider that this band implied in the emission properties corresponds to a  $\pi-\pi^*$  transition. The nature of the first excited state will be further discussed in terms of the results of MO calculations.

The natural lifetimes are also listed in Table 1. Due to the lower values of the absorptivities the values are significantly large in comparison with the values obtained for the phenoxathiin derivative.

**Table 1. Parameters of the absorption spectrum.**

Solvent	$\nu$ ( $\text{cm}^{-1}$ )	$\epsilon$ ( $\text{M}^{-1} \text{cm}^{-1}$ )	$\tau_0$ (ns)
CHX	30478	481	78
$\text{CH}_3\text{OH}$	29584	471	103

The fluorescence spectra in several solvents with different polarity are presented in Fig. 2 and some photophysical properties are listed in Table 2.

The emission maxima are located in the range of  $22000 \div 18000 \text{ cm}^{-1}$  ( $\lambda_F = 455 \div 555 \text{ \AA}$ ) and are strongly dependent on the solvent polarity indicating a change in the charge density distribution in the excited state.

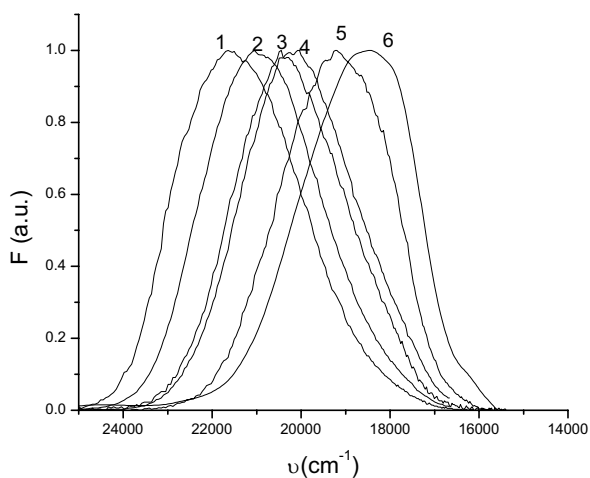


Fig. 2: Emission spectra of 1 in several solvents:  
1) CHX; 2) dioxane; 3) n-Butanol; 4) DMSO; 5) ACN; 6) Methanol.

**Table 2. Photophysical properties of the excited state**

Solvent	$\nu_F$ ( $\text{cm}^{-1}$ )	FWHM ( $\text{cm}^{-1}$ )	$\Delta\nu^*$ ( $\text{cm}^{-1}$ )	$\nu_{00}$ ( $\text{cm}^{-1}$ )	$\Delta\nu_1^{**}$ ( $\text{cm}^{-1}$ )	$\phi$
CHX	21598	2762	8880	25000	3402	0.06
DMSO	20449	2602	9392	25063	4614	0.11
ACN	20080	2643	10041	24392	4310	0.17
$\text{C}_2\text{H}_5\text{OH}$	19305	2546	10344	23365	4060	0.09
$\text{CH}_3\text{OH}$	18450	2440	11134	24331	5881	0.03

\* Stokes shift,  $\Delta\nu = \nu_A - \nu_F$

\*\* Stokes loss  $\Delta\nu = \nu_{0,0} - \nu_F$

The increase in the dipole moment value in the excited state,  $\Delta\mu$ , was estimated using the dependence of either the fluorescence wavenumber,  $\nu_F$ , (eq. 1) or the Stokes shift,  $\Delta\nu$ , (eq. 2,3) on some solvent polarisation functions, the Lippert-Mataga [11,12] model and the  $E_T^N$  solvent parameter given by Reichardt [13÷15].

In the Lippert-Mataga equations,  $\rho$  represents the radius of the solvent cavity and  $n$  and  $\varepsilon$  the refractive index and the dielectric constant of the solvent.

$$\nu_F = \nu_{F0} - \frac{2\Delta\mu^2}{ch\rho^3} \left( \frac{\varepsilon-1}{2\varepsilon+1} - \frac{1}{2} * \frac{n^2-1}{2n^2+1} \right) \quad (1)$$

$$\Delta\nu = \frac{2\Delta\mu^2}{ch\rho^3} \left( \frac{\varepsilon-1}{2\varepsilon+1} - \frac{n^2-1}{2n^2+1} \right) \quad (2)$$

The plot  $\nu_F$  vs  $f(\varepsilon, n)$  is presented in Fig. 3. Considering the slope of the plot and two limit values for the radius of the cavity,  $\rho=4.0$  Å and  $\rho=4.8$  Å we have obtained an increase of the dipole moment,  $\Delta\mu$ , of 6.3 D and 9.2 D, respectively. The last value was obtained considering 40 % of the average value of the larger molecular diameter [16]. The second plot (eq. 2) led to similar although somewhat lower values.

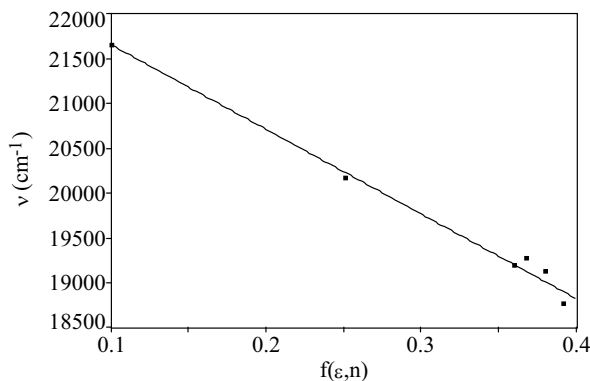


Fig. 3: Lippert-Mataga plot,  $\nu_F$  vs  $f(\varepsilon, n)$ , eq.(1).

In the third method,

$$\Delta\nu = 11307,6 * \frac{\Delta\mu^2}{\Delta\mu_{ref}^2} * \left( \frac{\rho_{ref}}{\rho_f} \right)^3 * E_T^N + \text{const} \quad (3)$$

$E_T^N$  is given in respect with the  $E_T(30)$  values for the solvent, water and TMS.

$$E_T^N = \frac{E_T(30)_{\text{solv}} - E_T(30)_{\text{TMS}}}{E_T(30)_{\text{water}} - E_T(30)_{\text{TMS}}}$$

The reference was the pyridinium N-phenoxyde betaine dye for which  $\Delta\mu = 9\text{D}$  and  $\rho = 6.2\text{\AA}$ . Plotting  $\Delta\nu$  vs  $E_T^N$  (eq.3) and using  $\rho = 4.8\text{\AA}$  the increase in the dipole moment,  $\Delta\mu$ , was significantly smaller, i.e.  $3.20\text{D}$ .

The differences obtained using the different polarity scales are very large. Two possible facts can account for this result: firstly, as was previously shown, the errors in the estimation of the position of the absorption bands which are present more as shoulder on the band at higher wavelengths and secondly, the presence of some specific interactions with the solvents not accounted for in the Lippert-Mataga model. If the only cause would be the errors in the experimental data on  $\nu_A$ , the differences using the two Lippert-Mataga equations would be larger. We consider that the value obtained using the  $E_T^N$  values reflect more adequately the change of the dipole moment upon excitation. Other literature data reported that the Reichardt-Dimroth polarity scale is more realistic as it takes also dispersive and specific (hydrogen bonding) interactions into account [17].

The experimental data evidenced a charge transfer character of the first excited state. However, the dipole moment increase in the excited state is smaller than that found for the phenoxathiin derivative, **III**. The presence of two sulphur atoms in the median heteroring, determines an enhanced delocalisation in the median heteroring and lower density charge on each sulphur atom; as the charge transfer implies mainly the sulphur atom in the para position in respect with the acceptor it is not unexpected a smaller charge transfer.

The fluorescence quantum yields are also listed in Table 2. The values of the quantum yields are situated between those of the other two related acetyl derivatives. The  $\nu_{0,0}$  value decreases in going from nonpolar towards the polar and protic solvents accounting for the enhanced influence of the solvent on the excited state solvation process. The same effect is reflected by the Stokes shift values.

The MO calculations on the ground and excited singlet and triplet states were performed in order to confirm on a theoretical basis the experimental findings on the ICT character of the excited state, to get information on the probability of an intersystem crossing (ISC) deactivation process, as the cause of the smaller quantum yield of **I** in respect with **III**.

The main results of the vacuum calculations for the ground ( $S_0$ ) and excited states ( $S_1$ ,  $T_1$ ) are collected in Table 3 and some relevant molecular orbitals are presented in Fig. 4. For the ground state the two in-plane conformers have the same stability while a difference was found for the excited states, the conformer **I-0** being more stable. The estimated rotation barriers are  $1.69\text{ kcal/mol}$  in the ground state,  $2.66/1.72\text{ kcal/mol}$  in  $S_1$  and  $2.88 / 1.91\text{ kcal/mol}$  in  $T_1$  for **I-0** and **I-180**, respectively.

The molecular orbitals are only slightly influenced by the conformation. The highest occupied molecular orbital,  $m$ , (Fig. 4b) is a  $\pi$  orbital mainly localized on the median heteroring, with a predominant contribution on the sulfur atoms (the coefficients of sulfur  $p_z$  atomic orbitals are  $\sim 0.5$ ). The shape of this orbital is similar with that in thianthrene, and its energy is in agreement with the experimental value of the ionization potential of the unsubstituted thianthrene,  $I = 7.94\text{ eV}$ . [18] This result points out the lack of the substituent

influence on this molecular orbital and explains the donor character of the thianthrene derivatives and their facility to give cation radicals and charge transfer complexes.

**Table 3. Heats of formation ( $\Delta H$  – kcal/mol) and dipole moments ( $D$ ) for the ground ( $S_0$ ) and excited states ( $S_1$  and  $T_1$ ) of the in-plane and orthogonal conformers of compound I. (vacuum calculations).  $\Delta E_{ST}$  ( $\text{cm}^{-1}$ ) represents the calculated singlet-triplet gap.**

	I-0		I-90		I-180	
	$\Delta H$	$\mu$	$\Delta H$	$\mu$	$\Delta H$	$\mu$
$S_0$	23.45	3.00	25.14	3.07	23.40	3.30
$S_1$ (C.I.=2)	71.20	3.95	73.86	3.42	72.14	4.63
$T_1$ (C.I.=2)	61.57	4.27	64.41	3.53	62.50	4.85
$\Delta E_{ST}$ (C.I.=2)	3378		3314		3381	
$S_1$ (C.I.=3)	71.11	3.70	73.84	3.35	72.06	4.52
$T_1$ (C.I.=3)	61.58	4.25	64.40	3.48	62.50	4.87
$\Delta E_{ST}$ (C.I.=3)	3342		3310		3353	

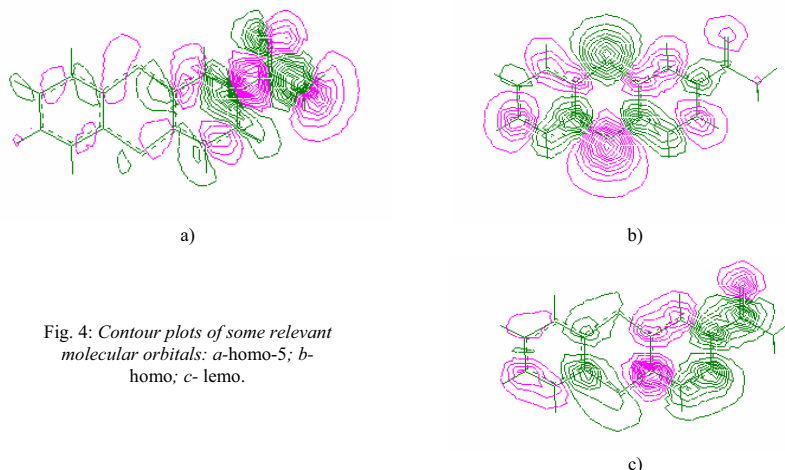


**Fig. 4: Contour plots of some relevant molecular orbitals: a- homo-5; b- homo; c- lomo.**

The lowest empty molecular orbital,  $m+1$ , (Fig. 4c) is also a  $\pi$  orbital but localized on the phenyl substituted ring and the acetyl group. The values of the atomic coefficients point out larger contributions for  $C_9$  and  $C_{12}$ , attesting an enhanced role of the sulfur atom in the para position with the substituent,  $S_{10}$ . The features of the frontier orbitals support the experimental observations on the  $\pi$ - $\pi^*$  nature of the first electronic transition. The in-plane orbital corresponding to the  $n$  electrons of the carbonylic oxygen atom, (Fig. 4a), is located at a lower energy, representing in fact the orbital  $m-4$ . Its energy has the same value as was found for other carbonyl containing compounds [1].

The same features of the molecular orbitals were obtained by the ab initio method using the basis STO-3G and STO-321G. The last basis leads to a value of the ionization potential close to that predicted by the AM1 method. The atomic populations in the highest occupied molecular orbital and in the orbital corresponding to the oxygen in-plane lone pair are given in Table 4.

**Table 4.** *Ab initio* MO energies and Mulliken atomic populations for two relevant molecular orbitals of conformer **I-0**: *m*, the highest occupied molecular orbital and *m-4*, the orbital corresponding mainly to the in-plane oxygen lone pair. (only atomic populations larger than 0.10 were considered).

Basis set	$\epsilon$ (eV)	<i>m</i>						$\epsilon$ (eV)	<i>m-4</i>		
		5	6	7(S)	8	9	10 (S)		12	16 (O)	17
STO-3G	-6.23	0.15	0.47	<b>0.47</b>	0.15	0.15	<b>0.47</b>	-9.03	0.29	<b>1.23</b>	0.29
STO-321G	-7.92	0.15	0.15	<b>0.52</b>	0.13	0.13	<b>0.47</b>	-11.40	0.30	<b>1.13</b>	0.30

It may be seen that the 2 electrons contained in homo are localized only on the central ring, the larger values being obtained on the sulphur atoms.

The dipole moment values are also included in Table 3. Several observation can be made: firstly, the dipole moment is dependent on the conformation, the larger values being obtained for **I-180**; secondly, the dependence is more pronounced for the excited states, especially for  $S_1$ ; the calculations predict an increase of  $\mu$  in the excited state but the increase is very low, only about 1-1.5 D. In comparison with the experimental estimations the calculated increase in the dipole moment is more close to the result obtained using the Reichardt-Dimroth polarity scale. It can also be seen that the first triplet is more polarised than the singlet. The ground state dipole moment calculated by the ab initio method using the basis set 3-21G is 3.16 D.

**Table 5.** Free energy of solvation (kcal/mol) for the ground and excited states of the three conformers in different solvents

	CHX			CH3OH		
	<b>I-0</b>	<b>I-90</b>	<b>I-180</b>	<b>I-0</b>	<b>I-90</b>	<b>I-180</b>
$S_0$	-14.31	-14.33	-14.16	-17.22	-17.19	-16.49
$S_1$	-9.65	-10.07	-9.68	-18.40	-18.19	-18.75
$T_1$	-9.94	-10.00	-9.92	-19.95	-18.47	-20.34
	ACN			DMSO		
	<b>I-0</b>	<b>I-90</b>	<b>I-0</b>	<b>I-90</b>	<b>I-0</b>	<b>I-90</b>
$S_0$	-17.42	-17.24	-17.42	-17.24	-17.42	-17.24
$S_1$	-18.61	-18.24	-18.61	-18.24	-18.61	-18.24
$T_1$	-20.17	-18.52	-20.17	-18.52	-20.17	-18.52

The solvation energies are listed in Table 5. It can be seen that the calculated values reflect the experimental trend on the solvatochromic effects of the solvents, as long as we don't consider the protic solvents. As the prediction of a bathochromic shift going from



cyclohexane towards the polar solvents is straightforward, the difference between the effects of DMSO and ACN, both polar and aprotic solvents, is not so evident. The results in Table 5 point out a lower solvation energy for dimethylsulphoxide as against acetonitrile in agreement with the lower wavelength emission maximum observed in this solvent. On the other part the solvatochromicity observed in the protic solvents is not accounted for by the theoretical model showing that some specific interactions, likely hydrogen bond formation, are also present.

The calculated singlet-triplet gap of about  $3300\div 3500\text{ cm}^{-1}$  is only slightly dependent on the solvent and on the orbitals implied in the configurational interactions. This value is lower than that obtained for the phenoxathiin derivative, **II** ( $5300\text{-}5600\text{ cm}^{-1}$ ) pointing out a higher probability for an intersystem crossing nonradiative deactivation pathway and accounting for the lower quantum yields.

## Conclusions

The experimental data on the emission spectrum of 2-acetyl-thianthrene, the positive solvatochromicity, the dependence of  $\nu_{0-0}$  and of the Stokes loss values on the solvent polarity point out the ICT character of the first excited state. Considering both the absorption and emission features we consider that the first excited state,  $S_1$  corresponds to a  $\pi\text{-}\pi^*$  transition, in agreement with the observations made for the related derivatives. The molecular orbital calculations support these conclusions. From the theoretical point of view, the ICT character of  $S_1$  is reflected by the increase in the dipole moment and the larger values of the solvation energies calculated for  $S_1$  in comparison with  $S_0$ . The calculated singlet-triplet gap accounts for the lower quantum yields of **I** as against **III** predicting an enhanced probability of an ISC process.

## REFERENCES

1. Ionescu, S., Gavrilu, D., Maior, O. and Hillebrand, M. (1999) *J.Photochem. Photobiol. A: Chemistry* **124**, 67-73.
2. Hillebrand, M., Gavrilu, D., Maior, O. and Tintaru, A. (1999) *Rev. Roum. Chimie* **44**, 569-576.
3. Rettig, W. (1986) *Angew. Chem. Int. Ed. Engl.* **25**, 971-988.
4. Van Auwerer, M., Grabovski, Z.R. and Rettig, W. (1991) *J. Phys. Chem.* **95**, 2083-2092.
5. Ianczewski, M and Dec, M. (1961) *Roczniki Chem.* **35**, 745-748.
6. Vasiliu, G., Cohn, E. and Maior, O. (1962) *Analele Univ. Buc.* **35**, 151-153.
7. Gilbert, A. and Bagott, J. (1991) **Essential of Molecular Photochemistry**, Blackwell Scientific Publications, Oxford, 98.
8. Schmidt, M.W., Baldrige, K.K., Boatz, J.A., Elbert, S.T., Gordon, M.S., Jensen, J.J., Koseki, S., Matsunaga, N., Nguyen, K.A., Su, S., Windus, T.L., Dupuis, M. and Montgomery, J.A. (1993) *J. Comput. Chem.* **14**, 1347.
9. Hawkins, G.D., Giesen, D.G., Lynch, G.C., Chambers, C.C., Rossi, I., Storer, J.W., Li, J., Rinaldi, D., Liotard, D.A., Cramer, C. J. and Truhlar, D.G. (1997) **AMSOL-version 6.5.3** University of Minnesota, Minneapolis.
10. Storer, J.W., Giesen, D.J., Crammer, C.J. and Truhlar, D.G. (1995) *J. Comput.-Aided Mol. Design* **9**, 87-110.

11. Lippert, E. (1955) *Z. Naturforsch.* **10a**, 541.
12. Mataga, N., Kaifu, Y. and Koizumi, M. (1956) *Bull. Chem. Soc. Jap.* **29**, 465.
13. Ravi, M., Samanta, A. and Radhakrishnan, T.P. (1994) *J. Phys. Chem.* **98**, 9133-9136.
14. Kumar, S., Jain, S.K. and Rastogi, R.C. (2001) *Spectrochimica Acta part A* **57**, 291-298.
15. Reichardt, C. (1979) *Angew. Chemie, Int. Edn. Engl.* **18**, 98-110.
16. van Dijk, S.I., Wiering, P.G., Groen, C.P., Brouwer, A.M., Verhoven, J.W., Schuddeboom, W. and Warman, J.M. (1995) *J. Chem. Soc., Faraday Trans.* **91**, 2107-2114.
17. Dey, J. and Dogra, S.K. (1994) *J. Phys. Chem.* **98**, 9133-9136.
18. Amato, M.E., Grassi, A., Irgolic, K.J., Pappalardo, G.C. and Radics, L. (1993) *Organometallics* **12**, 775-780.